Curvature-driven transport of thin Bingham fluid layers in airway bifurcations

Cyril Karamaoun, Haribalan Kumar, Médéric Argentina, Didier Clamond, Benjamin Mauroy

Letter

Curvature-driven transport of thin Bingham fluid layers in airway bifurcations

Cyril Karamaoun,[1,2,3] Haribalan Kumar,[4] Médéric Argentina,[3,5] Didier Clamond,[2,3] and Benjamin Mauroy[2,3,*]

[1]*Sorbonne Université, CNRS, Laboratoire Jacques-Louis Lions (LJLL), F-75005 Paris, France*
[2]*Université Côte d'Azur, CNRS, LJAD, France*
[3]*Université Côte d'Azur, VADER Center, France*
[4]*Auckland Bioengineering Institute, Auckland, New Zealand*
[5]*Université Côte d'Azur, CNRS, INPHYNI, France*

(Received 30 August 2022; accepted 13 June 2024; published 7 August 2024)

The mucus on the bronchial wall forms a thin layer of non-Newtonian fluid, protecting the lungs by capturing inhaled pollutants. Due to the corrugation of its interface with air, this layer is subject to surface tension forces that affect its rheology. This physical system is analyzed using lubrication theory and three-dimensional simulations. We characterize the nonlinear behavior of the mucus and show that surface tension effects can displace overly thick mucus layers in airway bifurcations. This movement can disrupt the mucociliary clearance and break the homogeneity of the layer thickness.

DOI: 10.1103/PhysRevFluids.9.L081101

As one of the central organs of respiration, the main functions of the lung are to bring oxygen from ambient air to the blood and to extract carbon dioxide from the body. The large exchange surface between the air and the blood, about 75–100 m^2 [1,2], is connected to the ambient air by a space-filling and multiscale network of airways. To perform its functions, the lung relies on several physical processes and on its treelike geometry. In the lung, the transport of oxygen and carbon dioxide is the most studied physical process [3,4]. However, other physical processes are involved, and some of them protect the integrity of the organ [1].

One of these mechanisms relies on a layer of non-Newtonian fluid coating the airways walls: The bronchial mucus [5]. The lung is a potential entry point for external contaminants—dust particles, chemicals, bacteria, viruses—that are constantly inhaled. The mucus traps contaminants and is transported toward the larynx, where it is either expelled or swallowed. Two main phenomena are responsible for mucus displacement [6]. First, ciliated cells located in the bronchial epithelium beat metachronously [7], with the cilia pushing the mucus toward the trachea. This phenomenon is called *mucociliary clearance* [6,8]. Second, during coughing [9,10] or at high ventilation rates [11], exhaled airflows can apply shear stress to the mucus that is high enough to induce its displacement. The efficiency of the protection by the mucus depends on the proper functioning of these two phenomena. Pathologies such as asthma, chronic obstructive pulmonary disease, or cystic fibrosis can impair mucociliary clearance, leading to major respiratory symptoms and to infections [12–14]. The mucociliary clearance and the air-mucus interaction have been explored thoroughly [9,11,15–21].

Other physical phenomena, such as gravity [22] and surface tension [23], can affect mucus transport. The role of surface tension on the air-mucus interface remains not well understood as

*Contact author: benjamin.mauroy@univ-cotedazur.fr

TABLE I. Data range of our model parameters and their default values used in this Letter, shown between parentheses.

Quantity	Value (reference value)	Notation	Ref.
	Lungs' geometrical data		
Trachea radius	0.01 m	r_0	[1]
Reduction factor	$(1/2)^{1/3} \sim 0.79$	h	[1,24,34]
	Mucus properties		
Surface tension	0.03 Pa m	γ	[25]
Mucus density	1000 kg m^3 (water)	ρ	[26]
Mucus viscosity	$10^{-3}-10$ Pa s (1)	μ	[27]
Mucus yield stress	$10^{-2}-10$ Pa (0.1)	σ_y	[27]
Mucus layer thickness (healthy)	5−30 μm (10)	τ	[16]
Cilia-induced mucus velocity	10−500 μm s^{-1} (50)	v_{cilia}	[28–30]

of today. The large airway curvatures suggest that the multiscaled structure of the bronchial tree, together with surface tension and mucus rheology, can affect the transport of mucus. However, in most studies, mucus is modeled as a Newtonian fluid [22,23,30–32].

Surface tension induces (Laplace) pressure jumps, Δp_L, across curved interfaces ($\Delta p_L = 2\gamma\kappa$, where γ is the surface tension coefficient and κ is the mean curvature of the interface). The distribution of this pressure can be evaluated in a self-similar tree model of the bronchial tree [1,3,24,33–35]. This model is a bifurcating tree with branches as perfect cylinders. The size of the branches decreases homothetically at each bifurcation by a factor $h = 2^{-1/3} \simeq 0.79$. In this model, the airways are indexed by their generation i, representing the number of bifurcations from the airway to the root of the tree (trachea). The radius of the airways in the ith generation is $r_i = h^i r_0$, with r_0 being the radius of the root of the tree. Assuming that the air-mucus interface and the airways have the same curvature, the Laplace pressure in the ith generation is $p_{L,i} = -\gamma/r_i$. This pressure decreases with the generation index, with curvature effects tending to push the layer toward the deeper parts of the tree. The resulting stress in a layer of thickness τ that coats the bifurcation between generations i and $i+1$ can be evaluated as $\sigma_i \simeq \gamma \frac{h-1}{r_i^2}\frac{\tau}{2}$ (see [36], Sec. I). This stress is larger in the small bifurcations, as it increases with the generation index. However, a more detailed analysis is needed to evaluate whether the curvature effects can effectively move the mucus. Therefore, detailed bifurcation shapes, more realistic mucus rheology, and mucus hydrodynamics must be included in the model.

Mucus is a complex viscoelastic fluid, potentially thixotropic [27]. Its rheological properties depend on the individual, the localization of the mucus in the bronchial tree, and the environmental factors such as air humidity and temperature. Mechanical constraints also influence mucus behavior, and one of its core properties is to exhibit a yield stress, σ_y, below which it behaves like a solid material [11,17–19,27]. This characteristic means that the internal shear stresses in the fluid must overcome σ_y for the mucus to behave like a fluid with viscosity μ. The typical healthy thickness τ of the mucus layer is on the order of 10 μm [29]. To understand under which conditions surface tension can be large enough to overcome the mucus yield stress, we modeled the mucus as a Bingham fluid. This approach has already provided valuable insights [17,18]. Moreover, it captures the layer's nonlinear dynamics, which cannot be well represented with a Newtonian fluid.

According to Table I, the Reynolds number is small in the mucus layer, $\text{Re} \sim \rho v_{\text{cilia}} \tau/\mu < 0.015$. Thus, fluid mechanics can be approximated using the Stokes equations. Denoting $\boldsymbol{u}$ as the fluid

velocity and p as the fluid pressure, the momentum and mass conservation equations write

$$\begin{aligned}
&\rho\frac{\partial \boldsymbol{u}}{\partial t} - \boldsymbol{\nabla}\cdot\Sigma + \nabla p = 0 && \text{in the layer}\\
&\boldsymbol{\nabla}\cdot\boldsymbol{u} = 0 && \text{in the layer}\\
&\Sigma\cdot\boldsymbol{n} - p\boldsymbol{n} = p_L\boldsymbol{n} && \text{at air-fluid interface } \mathcal{L}_t\\
&\boldsymbol{u} = 0 && \text{at airway wall } W\\
&\frac{\mathrm{d}\boldsymbol{x}}{\mathrm{d}t} = [\boldsymbol{u}(\boldsymbol{x},t)\cdot\boldsymbol{n}(\boldsymbol{x},t)]\boldsymbol{n}(\boldsymbol{x},t) && \boldsymbol{x}\in\mathcal{L}_t\\
&p_L = -2\gamma\kappa(\boldsymbol{x},t) && \boldsymbol{x}\in\mathcal{L}_t
\end{aligned}$$

Here, $\boldsymbol{n}(\cdot,t)$ represents the normal to the air-Bingham fluid interface $\mathcal{L}_t$ at time t, and κ denotes the mean curvature of this interface. The normals are oriented toward the air medium, and the characteristic thickness of the layer along these normals is denoted by τ. Σ is the viscous stress tensor. The air-Bingham fluid interface $\mathcal{L}_t$ is a free surface, and a geometric point $\boldsymbol{x}$ on its surface moves with the normal component of the Bingham layer velocity, $[\boldsymbol{u}(\boldsymbol{x})\cdot\boldsymbol{n}(\boldsymbol{x})]\boldsymbol{n}(\boldsymbol{x})$. Mucociliary clearance could be modeled with a slip boundary condition on the wall W. However, to isolate the sole effects of surface tension, clearance is not considered in the model, and a nonslip boundary condition is assumed on W.

The Bingham fluid constitutive equations are

$$\begin{aligned}
&\Sigma = \left(\mu + \frac{\sigma_y}{\dot\gamma}\right)\dot\Gamma \quad \text{for } \sigma > \sigma_y\\
&\dot\Gamma = 0 \quad \text{for } \sigma \leqslant \sigma_y
\end{aligned}$$

with $\dot\Gamma = \frac{1}{2}[\boldsymbol{\nabla}u + (\boldsymbol{\nabla}u)^{\mathrm{t}}]$ the rate of strain tensor and with $\sigma = \sqrt{\frac{1}{2}\Sigma{:}\Sigma}$ and $\dot\gamma = \sqrt{\frac{1}{2}\dot\Gamma{:}\dot\Gamma}$ the second invariants of, respectively, the stress tensor and the rate of strain tensor.

Given that the mucus layer is generally thin compared to the mean curvature radius of the bronchial wall, planar lubrication theory applies [37,38] (see [36], Sec. II). Our results show that the viscous stresses tangential to the wall dominate inside the fluid. These stresses are proportional to the interface curvature gradient $\nabla_\xi\,\kappa$, computed in the curvilinear coordinate system $\boldsymbol{\xi}$. The normal stress is dominated by the Laplace pressure. Our theory uncovers a characteristic Bingham-like number $B = \frac{\sigma_y r^2}{2\gamma\tau}$, where r is the characteristic radius of curvature of the interface, typically the radius of the airway. The fluid layer remains liquid if $B < \|\nabla_{\tilde\xi}\,\tilde\kappa\|$, where $\nabla_{\tilde\xi}\,\tilde\kappa = r^2\times\nabla_\xi\,\kappa$ (quantities with tildes are normalized by r).

A proportion $e = \max(0, 1 - B/\|\nabla_{\tilde\xi}\,\tilde\kappa\|)$ of the layer near the wall is liquid [17,18]. Above this liquid layer, the Bingham fluid is solid. The liquid layer drags the solid one. The surface tension homogenizes the layer thickness, thus we assume hereafter that τ is constant and that the layer curvature equals that of the airways (this analysis assumes the airways are perfectly smooth). Thus, we do not account for large fluid accumulations, clots, or plugs [17–19,39]. Under these conditions, for the ith generation and to the leading order, the velocity field $\boldsymbol{v}_{\mathrm{st},i}$ (averaged over the layer thickness) is

$$\begin{aligned}
&\boldsymbol{v}_{\mathrm{st},i} = -f(e_i)\,\frac{\gamma\tau^2}{\mu r_i^2}\,\nabla_{\tilde\xi}\,\tilde\kappa, \quad f(e) = e^2\Big(1 - \frac{e}{3}\Big),\\
&e_i = \max\left(0, 1 - \frac{B_i}{\|\nabla_{\tilde\xi}\,\tilde\kappa\|}\right).
\end{aligned} \tag{1}$$

The vector $-\frac{\gamma\tau^2}{\mu r_i^2}\nabla_{\tilde\xi}\,\tilde\kappa$ represents the velocity in the case of a Newtonian fluid. Our results show the presence of a prefactor $f(e_i)$ in the case of a non-Newtonian fluid. This dimensionless prefactor fully characterizes the non-Newtonian behavior and depends nonlinearly on the Bingham number B_i in the ith generation.

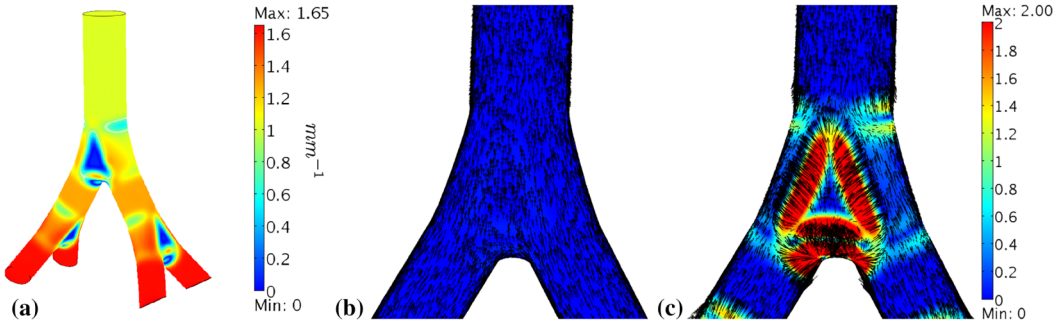

FIG. 1. (a) The reference 3D geometry used with the lubrication theory. The geometry is rescaled to cover all the scales of the bronchial tree bifurcations. The root branch radius is 1 mm. The branches size decreases with a ratio $h = (1/2)^{1/3}$ at the bifurcations. The branching angle is 60°, and the angle between the two successive branching planes is 90°, in accordance with the mean observed values [34]. The colors represent twice the nonsigned mean curvature field $|\kappa_0|$ (m^{-1}). (b) ($\tau = 10$ μm); (c) ($\tau = 75$ μm): Bingham fluid velocity fields $\boldsymbol{v}_{m,i}$ (arrows) and the ratio α between the amplitudes of the velocity induced by surface tension effects and the velocity induced by the idealized mucociliary clearance, i.e., $\alpha = \|\boldsymbol{v}_{\mathrm{st},i}\|/\|\boldsymbol{v}_{\mathrm{cilia}}\|$ (colors). Here, the mother branch has a radius of 1 mm and the daughter branches a radius of $(1/2)^{1/3} \simeq 0.79$ mm. At physiological thickness (b), only the idealized mucociliary clearance drives the motion of the mucus. For nonhealthy thickness (c), the idealized mucociliary clearance is strongly altered by surface tension effects.

Due to the scaling law between generations, the mean curvature gradients in the ith generaton are $\nabla_{\tilde{\xi}^i}\kappa_i = h^{-2i} r_0^{-2} \nabla_{\tilde{\xi}} \tilde{\kappa}$. This leads to a scaling law for the fluid velocity:

$$\boldsymbol{v}_{\mathrm{st},i} = \left(\frac{1}{h^2}\right)^i f(e_i)\, \frac{\gamma \tau^2}{\mu {r_0}^2} \nabla_{\tilde{\xi}} \tilde{\kappa}. \tag{2}$$

In addition, the wall mean curvature $\tilde{\kappa}$ is obtained from an idealized three-dimensional (3D) tree geometry, see Fig. 1(a) and [36], Sec. IV. The fluid velocity field in the 3D idealized tree is obtained from the theoretical formula (1). Finally, the velocity induced by mucociliary clearance is also evaluated in the 3D idealized tree. It is modeled as the gradient of a Laplacian field on the bifurcation walls (see [36], Sec. V). The resulting idealized clearance is tangential to the bifurcation walls and directed toward the larger airways [30]. Its amplitude is set to 50 μm s^{-1} [29].

Many common lung pathologies induce a thickening of the layer [40]. Therefore, in addition to healthy mucus layer thickness, other thicknesses compatible with mucus pathophysiology were tested. Typical velocity outputs of this study are presented in Fig. 1 (spatial distribution) and Fig. 2(a) (averaged amplitude). Our results show that after a threshold generation, the curvature gradients are able to overcome the yield stress of the Bingham fluid. This implies that, from this generation onward, the fluid exhibits a liquid behavior and can be displaced. For healthy mucus ($\tau = 10$ μm), this threshold is around the ninth generation, see Fig. 2(a). In this case, the velocity magnitude is negligible compared to that induced by mucociliary clearance. For thicker layers, the threshold generation decreases and the velocity increases, eventually becoming larger than the magnitude of the velocity induced by idealized clearance, see Fig. 2(a). Thus, the thicker the mucus, the more the idealized clearance is impaired (see Fig. 1). Eventually, the effects of the clearance vanish, and the velocity field is driven solely by curvature effects, see Fig. 1(c).

The disruption of the clearance depends on the layer thickness and the position in the bifurcation. The convergence (or divergence) of the predicted velocity field indicates possible mucus accumulation (or depletion) at different spots in the bifurcation, see Fig. 1(c). A local accumulation increases the risk of bronchial obstruction. Conversely, a local depletion reduces the protection of the epithelium, making it more susceptible to external contaminants and physicochemical stresses [41]. Furthermore, our model suggests that local mucus accumulation is likely to develop first in

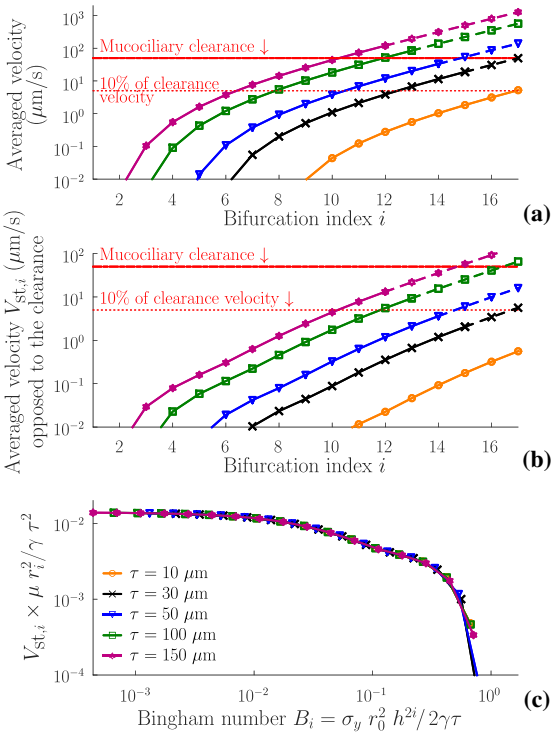

FIG. 2. Velocity patterns with parameter values $\sigma_y = 0.1$ Pa, $\mu = 1$ Pa s and a clearance amplitude of 50 μm s^{-1}. The dashed parts of the curves correspond to generations where the model hypothesis $\tau/r_i \ll 1$ loses its validity (i.e., $\tau/r_i > 10\%$). Our results show that curvature effects can disrupt mucociliary clearance for pathological thicknesses of the layer ($\tau \geqslant 50$ μm), particularly in the medium and small airways. (a) Bingham layer velocity amplitude (curvature effects only) averaged over the bifurcation and layer thickness. (b) Component of the Bingham layer velocity (curvature effects only) in the direction of the idealized clearance and averaged over the bifurcation and layer thickness. The average velocity induced by curvature effects is always opposed to clearance. (c) Averaged velocity opposed to clearance, normalized by the velocity of a Newtonian fluid in the same configuration. The normalized velocity depends only on the Bingham number B_i.

the parts of the airways closest to the bifurcation zone, see Fig. 1(c). On the other hand, the carina of the bifurcation, i.e., the meeting point of the two small airways, is more susceptible to mucus depletion since it has relatively low curvature, see Fig. 1(a). Notably, inhaled particles are more likely to deposit at the carina [42,43], and mucus overproduction might, counterintuitively, increase the risk of epithelial damage near the carina [42].

To quantify how the curvature gradient opposes the mucociliary clearance in a bifurcation, we project the velocity field $v_{\mathrm{st},i}$ (induced by surface tension) onto the local direction of the idealized clearance. Then, we average this velocity component over the layer thickness and the bifurcation to define $V_{\mathrm{st},i}$ (see [36], Sec. III). The results are shown in Figs. 2(b) and 2(c). In all the cases, the averaged Bingham fluid velocity opposes that induced by the idealized clearance. Moreover, the non-Newtonian effects are driven only by the Bingham number $B_i = \frac{\sigma_y r_i^2}{2\gamma\tau}$, as shown in Fig. 2(c). For $B_i < 0.1$, the fluid behaves as a liquid throughout the entire tree and the curvature effects most strongly counteract the clearance. For $B_i > 0.5$, the velocities drop drastically, and the clearance is no longer disrupted; in this case, the Bingham fluid is no longer fully liquid and eventually behaves as a solid.

These results agree with observations, as an increased thickness of the mucus layer in pathological conditions has been associated with a disturbance of clearance [12–14]. Moreover, our analysis highlights the importance of the mechanisms that control mucus thickness, particularly in the bifurcations [29].

In the absence of clearance, the fluid in the bifurcation is globally driven by capillarity toward the small airways, as shown in Fig. 2(b). This movement opposes that induced by clearance. Curvature gradients vanish in cylindrical airways, and further mucus displacement along the small airways can only result from a nonconstant thickness of the layer. Surface tension effects tend to homogenize the layer thickness until the shear stress falls below the yield stress, resulting in local accumulation of mucus. Thus, our analysis suggests that clearance can also compensate for curvature effects on the mucus in bifurcations. Moreover, the curvature gradients trigger the displacement of the layer mainly along the wall, indicating their contribution to maintaining a layer with constant thickness. However, when the layer is too thick, the curvature gradients become too strong for clearance to counteract these effects.

Our analysis reveals curvature effects on a Bingham fluid layer coating the airways walls of a bifurcation. Our results suggest that a pathological thickening of the bronchial mucus layer can counteract and potentially disrupt mucociliary clearance. However, the curvature effects on the mucus remain intricate, and the model does not account for the full complexity of the bronchial mucus layer.

The rheology of mucus remains incompletely understood [44], with properties varying widely between individuals and influenced by environmental factors [27,44]. Therefore, our results are primarily qualitative and not exhaustive. However, employing a Bingham model to represent mucus allows one to capture its key properties, such as viscosity and yield stress [27,44], and our predictions align with lung pathophysiology [12–14].

The thickness of mucus likely varies depending on the location within the bronchial tree [29]. Moreover, bronchi are not perfect cylinders, and their wall curvature is not constant. These phenomena, which are not considered in our model, can influence the layer thickness.

Our study demonstrates that curvature effects can displace thick layers of Bingham fluid in airways bifurcations. In the context of lung pathologies, our findings suggest that curvature effects likely play a significant role in disrupting the mucociliary clearance when mucus accumulation is present. This work paves the way to a deeper understanding of bronchial mucus dynamics in pathological lungs. Future research should incorporate more realistic models of the bronchial tree and air-mucus interface, as well as consider other biophysical phenomena such as gravity [22], to assess their respective impacts. Moreover, our work highlights the possibility of "hidden" physical processes being triggered by certain pathologies, significantly affecting organs' function.

This work has been supported by the Mission pour l'Interdisciplinarité du CNRS, the Agence Nationale de la Recherche (the VirtualChest project, ANR-16-CE19-0014; the IDEX UCA JEDI, ANR-15-IDEX-01), the Académie des Systèmes Complexes de l'Université Côte d'Azur and the Association Vaincre La Mucoviscidose (RF20190502489).

[1] E. R. Weibel, *The Pathway for Oxygen: Structure and Function in the Mammalian Respiratory System* (Harvard University Press, Cambridge, MA, 1984).

[2] J. B. West, *Respiratory Physiology: The Essentials*, 9th revised edition (Lippincott Williams and Wilkins, Philadelphia, 2011).

[3] F. Noël, C. Karamaoun, J. A. Dempsey, and B. Mauroy, The origin of the allometric scaling of lung ventilation in mammals, Peer Commun. J. **2**, e2 (2022).

[4] B. Sapoval, M. Filoche, and E. R. Weibel, Smaller is better—but not too small: A physical scale for the design of the mammalian pulmonary acinus, Proc. Natl. Acad. Sci. USA **99**, 10411 (2002).

[5] J. V. Fahy and B. F. Dickey, Airway mucus function and dysfunction, N. Engl. J. Med. **363**, 2233 (2010).
[6] M. King, Physiology of mucus clearance, Paediatr. Respir. Rev. **7**, S212 (2006).
[7] S. Chateau, J. Favier, S. Poncet, and U. D'Ortona, Why antiplectic metachronal cilia waves are optimal to transport bronchial mucus, Phys. Rev. E **100**, 042405 (2019).
[8] X. M. Bustamante-Marin and L. E. Ostrowski, Cilia and mucociliary clearance, Cold Spring Harbor Perspect. Biol. **9**, a028241 (2017).
[9] P. J. Basser, T. A. McMahon, and P. Griffith, The mechanism of mucus clearance in cough, J. Biomech. Eng. **111**, 288 (1989).
[10] P. T. MacKlem, Physiology of cough, Ann. Otol. Rhinol. Laryngol. **83**, 761 (1974).
[11] J. Stéphano and B. Mauroy, Wall shear stress distribution in a compliant airway tree, Phys. Fluids **33**, 031907 (2021).
[12] M. Del Donno, D. Bittesnich, A. Chetta, D. Olivieri, and M. T. Lopez-Vidriero, The effect of inflammation on mucociliary clearance in asthma: An overview, Chest **118**, 1142 (2000).
[13] J. T. Ito, D. Ramos, F. M. M. Rodrigues, R. F. Xavier, M. R. Leite, J. Nicolino, G. N. B. Ferrari, A. C. Toledo, and E. M. C. Ramos, Impairment of mucociliary clearance in COPD and smokers: Same or different? Eur. Resp. J. **40**(Suppl. 56), 1056 (2012).
[14] M. Robinson and P. T. B. Bye, Mucociliary clearance in cystic fibrosis, Pediatric Pulmonology **33**, 293 (2002).
[15] S. Gsell, E. Loiseau, U. D'Ortona, A. Viallat, and J. Favier, Hydrodynamic model of directional ciliary-beat organization in human airways, Sci. Rep. **10**, 8405 (2020).
[16] C. Karamaoun, B. Haut, and A. Van Muylem, A new role for the exhaled nitric oxide as a functional marker of peripheral airway caliber changes: A theoretical study, J. Appl. Physiol. **124**, 1025 (2018).
[17] B. Mauroy, C. Fausser, D. Pelca, J. Merckx, and P. Flaud, Toward the modeling of mucus draining from the human lung: Role of the geometry of the airway tree, Phys. Biol. **8**, 056006 (2011).
[18] B. Mauroy, P. Flaud, D. Pelca, C. Fausser, J. Merckx, and B. R. Mitchell, Toward the modeling of mucus draining from human lung: Role of airways deformation on air-mucus interaction, Front. Physiol. **6**, 214 (2015).
[19] J. Stéphano and B. Mauroy, Modeling shear stress distribution in a deformable airway tree, *27th Canadian Congress of Applied Mechanics* (Sherbrooke, Canada, 2019).
[20] L. Xu and Y. Jiang, Mathematical modeling of mucociliary clearance: A mini-review, Cells **8**, 736 (2019).
[21] J. M. Zahm, M. King, C. Duvivier, D. Pierrot, S. Girod, and E. Puchelle, Role of simulated repetitive coughing in mucus clearance, Eur. Respir. J. **4**, 311 (1991).
[22] F. Romanò, M. Muradoglu, and J. B. Grotberg, Effect of surfactant in an airway closure model, Phys. Rev. Fluids **7**, 093103 (2022).
[23] O. Erken, F. Romanò, J. Grotberg, and M. Muradoglu, Capillary instability of a two-layer annular film: An airway closure model, J. Fluid Mech. **934**, A7 (2022).
[24] B. Mauroy, M. Filoche, E. R. Weibel, and B. Sapoval, An optimal bronchial tree may be dangerous, Nature (London) **427**, 633 (2004).
[25] R. Hamed and J. Fiegel, Synthetic tracheal mucus with native rheological and surface tension properties, J. Biomed. Mater. Res. **102**, 1788 (2014).
[26] J. A. Ohar, J. F. Donohue, and S. Spangenthal, The role of guaifenesin in the management of chronic mucus hypersecretion associated with stable chronic bronchitis: A comprehensive review, J. COPD Found. **6**, 341 (2019).
[27] S. K. Lai, Y.-Y. Wang, D. Wirtz, and J. Hanes, Micro- and macrorheology of mucus, Adv. Drug Delivery Rev. **61**, 86 (2009).
[28] G. R. Fulford and J. R. Blake, Muco-ciliary transport in the lung, J. Theor. Biol. **121**, 381 (1986).
[29] C. Karamaoun, B. Sobac, B. Mauroy, A. Van Muylem, and B. haut, New analysis of the mechanisms controlling the bronchial mucus balance, *27th Canadian Congress of Applied Mechanics* (Sherbrooke, Canada, 2019).

[30] M. Manolidis, D. Isabey, B. Louis, J. B. Grotberg, and M. Filoche, A macroscopic model for simulating the mucociliary clearance in a bronchial bifurcation: The role of surface tension, J. Biomech. Eng. **138**, 121005 (2016).
[31] P.-G. de Gennes, F. Brochard-Wyart, and D. Quéré, *Capillarity and Wetting Phenomena: Drops, Bubbles, Pearls, Waves* (Springer, New York, NY, 2004).
[32] H. R. Ogrosky, Impact of viscosity ratio on falling two-layer viscous film flow inside a tube, Phys. Rev. Fluids **6**, 104005 (2021).
[33] B. Sobac, C. Karamaoun, B. Haut, and B. Mauroy, Allometric scaling of heat and water exchanges in the mammals' lung, arXiv:1911.11700.
[34] M. H. Tawhai, P. Hunter, J. Tschirren, J. Reinhardt, G. McLennan, and E. A. Hoffman, CT-based geometry analysis and finite element models of the human and ovine bronchial tree, J. Appl. Physiol. **97**, 2310 (2004).
[35] E. R. Weibel, *Morphometry of the Human Lung* (Springer-Verlag, Berlin, Heidelberg, 1963).
[36] See Supplemental Material at http://link.aps.org/supplemental/10.1103/PhysRevFluids.9.L081101 for details about the mathematical and numerical computations.
[37] N. J. Balmforth and R. V. Craster, A consistent thin-layer theory for Bingham plastics, J. Non-Newtonian Fluid Mech. **84**, 65 (1999).
[38] R. L. Panton, *Incompressible Flow* (Wiley-Blackwell, Hoboken, NJ, 2013), pp. 198–219.
[39] J. B. Grotberg, Respiratory fluid mechanics and transport processes, Annu. Rev. Biomed. Eng. **3**, 421 (2001).
[40] O. W. Williams, A. Sharafkhaneh, V. Kim, B. F. Dickey, and C. M. Evans, Airway mucus, from production to secretion, Am. J. Respir. Cell. Mol. Biol. **34**, 527 (2006).
[41] C. Karamaoun, B. Haut, G. Blain, A. Bernard, F. Daussin, J. Dekerle, V. Bougault, and B. Mauroy, Is airway damage during physical exercise related to airway dehydration? Inputs from a computational model, J. Appl. Physiol. **132**, 1031 (2022).
[42] I. Balásházy, W. Hofmann, and T. Heistracher, Local particle deposition patterns may play a key role in the development of lung cancer, J. Appl. Physiol. **94**, 1719 (2003).
[43] J. R. Zierenberg, D. Halpern, M. Filoche, B. Sapoval, and J. B. Grotberg, An asymptotic model of particle deposition at an airway bifurcation, Math. Med. Biol. **30**, 131 (2013).
[44] M. Jory, D. Donnarumma, C. Blanc, K. Bellouma, A. Fort, I. Vachier, L. Casanellas, A. Bourdin, and G. Massiera, Mucus from human bronchial epithelial cultures: Rheology and adhesion across length scales, Interface Focus **12**, 20220028 (2022).